Particle-number conserving analysis of the high-K multi-quasiparticle bands in ^{179}Re*

ZHANG Zhen-Hua(张振华)[1;1)] XU Hong-Qiao(徐红巧)[2] SUN Bao-Xi(孙宝玺)[2]

[1] Institute of Theoretical Physics, Chinese Academy of Sciences, Beijing 100190, China
[2] Institute of Theoretical Physics, College of Applied Sciences, Beijing University of Technology, Beijing 100124, China

Abstract The experimentally observed ten rotational bands in ^{179}Re are analyzed with the particle-number conserving method for treating the cranked shell model with pairing interaction, in which the blocking effects are taken into account exactly. The experimental moments of inertia of these bands are reproduced quite well by our calculations with no free parameter and the deformation driving effects are discussed. The bandhead energies and the variation in the occupation probability of each cranked orbital are also analyzed.

Key words multi-quasiparticle band, moment of inertia, blocking effect, particle-number conserving method

PACS 21.60.-n, 21.60.Cs, 23.20.Lv

1 Introduction

In recent years, a lot of low-lying excited rotational bands with intrinsic multi-quasiparticle (qp) states have been observed [1–3]. For the well-deformed rare-earth nuclei with $A \sim 180$ ($Z \sim 74$, $N \sim 104$), the single-particle spectrum is dominated by high-Ω (projection of angular momentum along the symmetry axis) orbitals near the Fermi surface, e.g., the proton orbitals $\pi\mathbf{7/2}^-[\mathbf{523}]$ (the boldface letter denotes the high-j intruder orbitals), $\pi 7/2^+[404]$, $\pi\mathbf{9/2}^-[\mathbf{514}]$, $\pi 5/2^+[402]$, and the neutron orbitals $\nu\mathbf{7/2}^+[\mathbf{633}]$, $\nu 5/2^-[512]$, $\nu 7/2^-[514]$, $\nu\mathbf{9/2}^+[\mathbf{624}]$, etc. This special situation gives rise to low-lying excited high-K multi-quasiparticle bands.

In the rare-earth region, there are many interesting phenomena, such as signature inversion [4, 5], deformation-driving characteristics of high-j intruder orbitals [6], etc. The Re ($Z = 75$) isotopes are located at the edge of the rare-earth region and many experiments have been done to investigate this transitional nuclide. Many features, such as configuration dependent deformations [7], signature inversion in doubly-odd Re nuclei [8], multi-quasiparticle K isomers and K forbidden transitions [3, 9, 10], have been investigated in detail. Also much research concerning the high-spin structure and band crossing phenomena of Re nuclei has been done [7, 9, 11, 12]. It is well known that in the rare-earth region the $\nu i_{13/2}$ is responsible for the first backbending ($\hbar\omega \sim 0.20$–0.30 MeV) and the $\pi h_{11/2}$ is responsible for the second backbending, which usually occurs in the very high-spin region ($\hbar\omega \sim 0.50$ MeV) [13]. In the transitional Re nuclide, the backbending frequency (ω_c) may be a little different for each band due to different deformations. A larger deformation would reduce the alignment gain and move the backbending to a higher frequency [7]. Some experiments that are used to investigate ^{179}Re have been done [3, 7] and the experimental data were recently reported in Ref. [12]. But until now there have only been scarce theoretical calculations available, so in this paper we use the particle-number conserving (PNC) method to investigate this nucleus. The particle-number is conserved from beginning to end and the blocking effects are taken into account exactly in our calculation.

In this paper, the experimental 1-qp, 3-qp and 5-qp bands in ^{179}Re [3, 11, 12] are analyzed using the particle-number conserving (PNC) method. Details of the PNC formalism are given in [14, 15]. For convenience, the main formulation used in the present calculation is presented in Sect. 2. The PNC analysis

Received 4 February 2010

* Supported by NSFC (10775012, 10875157, 10979066), MOST (973 project 2007CB815000) and KIP of CAS (KJCX3-SYW-N02, KJCX2-YW-N32)

1) E-mail: zhzhang@itp.ac.cn

for the low-lying 1-qp and multi-quasiparticle bands in ^{179}Re, including the bandhead energies, moments of inertia (MOIs) and occupation probability of each cranked Nilsson orbital are given in Sect. 3. Sect. 4 gives a brief summary.

2 A brief review of the PNC method for the CSM with pairing interaction

The CSM Hamiltonian of an axially symmetric nucleus in the rotating frame is [14, 15]

$$\begin{aligned} H_{\rm CSM} &= H_0 + H_{\rm P}, \\ H_0 &= H_{\rm Nil} - \omega J_x. \end{aligned} \tag{1}$$

$H_0 = H_{\rm Nil} - \omega J_x$ is the one-body part of $H_{\rm CSM}$, where $H_{\rm Nil}$ is the Nilsson Hamiltonian, $-\omega J_x$ is the Coriolis interaction with cranking frequency ω about the x axis (perpendicular to the nuclear symmetry z axis). $H_{\rm P}$ is the pairing interaction

$$H_{\rm P} = -G\sum_{\xi\eta} a^+_{\xi} a^+_{\bar{\xi}} a_{\bar{\eta}} a_{\eta}, \tag{2}$$

where $\bar{\xi}$ ($\bar{\eta}$) labels the time-reversed state of the Nilsson state ξ (η) and G is the effective strength of pairing interaction, which is determined by the experimental odd-even difference in binding energies, and it is not a free parameter.

In the PNC calculation, a cranked many-particle configuration (CMPC) truncation (Fock space truncation) is used instead of the single-particle level (SPL) truncation in common shell-model calculations. This is crucial to make the PNC calculations for low-lying excited states both workable and sufficiently accurate [16, 17]. The stability of the calculations using the Fock space truncation has been investigated in detail by the Dudek group [17].

An eigenstate of $H_{\rm CSM}$ can be written as

$$|\psi\rangle = \sum_i C_i |i\rangle \qquad (C_i \,\text{real}), \tag{3}$$

where $|i\rangle$ is a CMPC (an eigenstate of the one-body operator H_0). In the following calculations, the CSM Hamiltonian (1) is diagonized in a sufficiently large CMPC space to obtain the solutions to low-lying excited eigenstates of $H_{\rm CSM}$. In the following calculation, the dimension of the CMPC space is about 700 for protons and 800 for neutrons. As we are only interested in the yrast and low-lying excited states, the numbers of important CMPCs involved (weight $> 1\%$) is very limited (usually < 20) and almost all of the CMPCs with weight $> 0.1\%$ are taken into account, so that the solutions to the low-lying excited states are accurate enough.

The kinematic moment of inertia for the state $|\psi\rangle$ is

$$\begin{aligned} J^{(1)} &= \frac{1}{\omega}\langle\psi|J_x|\psi\rangle \\ &= \frac{1}{\omega}\left(\sum_i C_i^2\langle i|J_x|i\rangle + 2\sum_{i<j} C_i C_j \langle i|J_x|j\rangle\right). \end{aligned} \tag{4}$$

The occupation probability n_μ of the cranked orbital $|\mu\rangle$ is $n_\mu = \sum_i |C_i|^2 P_{i\mu}$, where $P_{i\mu} = 1$ if $|\mu\rangle$ is occupied in $|i\rangle$, and $P_{i\mu} = 0$ otherwise.

It is noted that because $R_x(\pi) = {\rm e}^{-{\rm i}\pi J_x}$ and $[J_x, J_z] \neq 0$, the signature scheme breaks the validity of K being a good quantum number. However, considering $[J_x, J_z^2] = 0$, we can construct the simultaneous eigenstates of $(R_x(\pi), J_z^2)$. Each $|i\rangle$ in (3) is chosen as a simultaneous eigenstate of (H_0, J_z^2). Walker and Draculis [1] pointed out that some forms of K-mixing must exist to enable K-forbidden transitions observed in many low-lying rotational bands of axially symmetric nuclei. However, by convention, K is still used as a convenient quantum number to describe the rotational bands of deformed spheroidal nuclei. In the PNC treatment of the CSM with Hamiltonian (1), the seniority (number of unpaired particles) is not a good quantum number either, due to the appearance of the antipairing Coriolis interaction. Moreover, though the total number of particles n $\left(=\sum_\mu n_\mu\right)$ keeps exactly constant, the occupation probability n_μ for each orbital μ may change with increasing rotational frequency ω.

3 Analysis of the low-lying rotational bands in ^{179}Re

3.1 Cranked Nilsson levels near the Fermi surface of ^{179}Re

The cranked Nilsson single-particle levels near the Fermi surface of ^{179}Re are calculated at first. In our calculations, the Nilsson parameters (κ, μ) and the deformation parameters ($\varepsilon_2 = 0.2325$, $\varepsilon_4 = 0.0385$) for protons and neutrons are taken from the Lund systematics [18, 19]. A little change in ε_2 is made in $K^\pi = 1/2^-$ ($\pi\mathbf{1/2}^-[\mathbf{541}]$) due to the deformation driving effects of this orbital in Re nuclei [7, 11] and a slight adjustment is made in (κ, μ) to reproduce the bandhead energies of the low-lying 1-qp bands in ^{179}Re. For protons, $\kappa_4 = 0.0626$, $\kappa_5 = 0.0649$, $\mu_4 = 0.609$ and $\mu_5 = 0.533$. For neutrons, $\kappa_5 = 0.0660$,

$\kappa_6 = 0.0620$, $\mu_5 = 0.440$, $\mu_6 = 0.350$, $\nu 1/2^-[521]$ is shifted upward by $0.04\hbar\omega_0$ and $\boldsymbol{\nu 9/2^+[624]}$ is shifted downward by $0.06\hbar\omega_0$. The change in μ will cause a change in the relative position of the Nilsson levels in the same N shell, and a change in κ will lead to the change in the relative position of the neighboring N shell. In our calculations, we consider the $N = 4,5$ major shell for protons and the $N = 5,6$ major shell for neutrons. The adjusted Nilsson level scheme is shown in Fig. 1. The effective pairing interaction strength is determined by the experimental odd-even differences in binding energy: $G_{\rm p} = 0.30$ MeV (protons) and $G_{\rm n} = 0.28$ MeV (neutrons). So there is no additional free parameter in our calculations.

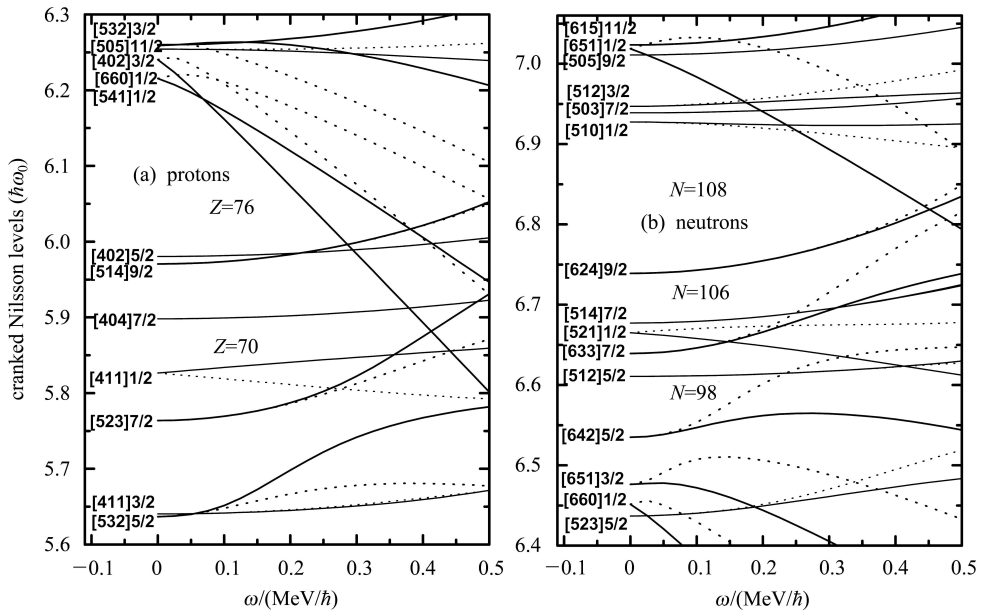

Fig. 1. The cranked Nilsson orbitals near the Fermi surface of ^{179}Re. The deformation parameters ($\varepsilon_2 = 0.2325, \varepsilon_4 = 0.0385$) are taken from the Lund systematics [18]. The Nilsson parameters κ and μ (Lund systematics [19]) are slightly adjusted to reproduce the bandhead energies of the low-lying 1-qp bands in ^{179}Re. (a) For protons, $\kappa_4 = 0.0626$, $\kappa_5 = 0.0649$, $\mu_4 = 0.609$ and $\mu_5 = 0.533$. (b) For neutron, $\kappa_5 = 0.0660$, $\kappa_6 = 0.0620$, $\mu_5 = 0.440$, $\mu_6 = 0.350$, $\nu 1/2^-[521]$ is shifted upward by $0.04\hbar\omega_0$ and $\boldsymbol{\nu 9/2^+[624]}$ is shifted downward by $0.06\hbar\omega_0$.

Table 1. Comparison of the experimental and calculated bandhead energies of 1-, 3- and 5-qp bands in ^{179}Re.

K^π	configuration*	$E_{\rm exp}$/keV	$E_{\rm cal}$/keV
$\frac{5}{2}^+$	$\pi\frac{5}{2}^+$	0	0
$\frac{9}{2}^-$	$\pi\boldsymbol{\frac{9}{2}}^-$	88	89
$\frac{15}{2}^-$	$\pi\boldsymbol{\frac{9}{2}}^-,\nu\frac{7}{2}^-,\nu\frac{1}{2}^-$	927	1520
$\frac{17}{2}^+$	$\pi\frac{5}{2}^+,\nu\frac{7}{2}^-,\nu\frac{5}{2}^-$	1815	1850
$\frac{19}{2}^+$	$\pi\boldsymbol{\frac{9}{2}}^-,\nu\boldsymbol{\frac{9}{2}}^+,\nu\frac{1}{2}^-$	1827	1770
$\frac{23}{2}^+$	$\pi\boldsymbol{\frac{9}{2}}^-,\nu\frac{7}{2}^-,\nu\boldsymbol{\frac{7}{2}}^+$	>1772	1697
$\frac{33}{2}^+$	$\pi\frac{5}{2}^+,\nu\boldsymbol{\frac{9}{2}}^+,\nu\frac{7}{2}^-,\nu\boldsymbol{\frac{7}{2}}^+,\nu\frac{5}{2}^-$	3456	3039
$\frac{33}{2}^-$	$\pi\boldsymbol{\frac{9}{2}}^-,\nu\frac{9}{2}^+,\nu\frac{7}{2}^-,\nu\boldsymbol{\frac{7}{2}}^+,\nu\frac{1}{2}^-$	3542	2709
$\frac{35}{2}^+$	$\pi\frac{7}{2}^+,\nu\boldsymbol{\frac{9}{2}}^+,\nu\frac{7}{2}^-,\nu\boldsymbol{\frac{7}{2}}^+,\nu\frac{5}{2}^-$	3703	3507

*Orbitals: protons (π): $\frac{5}{2}^+$: $\frac{5}{2}^+[402]$, $\frac{7}{2}^+$: $\frac{7}{2}^+[404]$, $\boldsymbol{\frac{9}{2}}^-$: $\boldsymbol{\frac{9}{2}}^-[\mathbf{514}]$. Neutrons ($\nu$): $\frac{7}{2}^-$: $\nu\frac{7}{2}^-[514]$, $\boldsymbol{\frac{9}{2}}^+$: $\boldsymbol{\frac{9}{2}}^+[\mathbf{624}]$, $\frac{1}{2}^-$: $\frac{1}{2}^-[521]$, $\boldsymbol{\frac{7}{2}}^+$: $\boldsymbol{\frac{7}{2}}^+[\mathbf{633}]$, $\frac{5}{2}^-$: $\frac{5}{2}^-[512]$.

Table 1 shows the experimental [3, 12] and calculated bandhead energies for 1-, 3- and 5-qp bands in ^{179}Re. Most of the experimental data can be well reproduced by the PNC calculation using the Nilsson level scheme and effective pairing strength (both for protons and neutrons) given above. So it seems reasonable for us to proceed with the following calculations. Some bandhead energies are not so well reproduced (e.g., $K^\pi = 15/2^+, 33/2^-$). They are also not very well reproduced in Ref. [3]. This may be due to configuration dependent deformation effects. In this transitional nuclide, the deformation in each rotational band is very complicated. If we consider these effects strictly, the results should be better, and this needs further investigation.

3.2 The MOIs and the backbending of the 1-qp bands in ^{179}Re

The experimental $J^{(1)}$s of the low-lying 1-qp bands in ^{179}Re [3, 11, 12] are shown in Fig. 2 by ■ ($\alpha = 1/2$) and □ ($\alpha = -1/2$), respectively. The PNC calculated $J^{(1)}$s for all of the low-lying 1-quasiproton bands are shown by solid ($\alpha = 1/2$) and dotted ($\alpha = -1/2$) lines. The experimental $J^{(1)}(\omega)$s are re-

produced quite well by the PNC calculations, which in turn confirms the assigned configurations for the 1-qp bands in ^{179}Re [3, 11, 12]. In Fig. 2(a), we see that reducing the quadrupole deformation ε_2 by a small amount ($\varepsilon_2 = 0.22$, reduced by about 6%), the backbending of the gsb $K^\pi = 5/2^+$ ($\pi 5/2^+[402]$) can be reproduced very well (dashed line). The alignment gain in the $\pi 5/2^+[402]$ band is larger than that gain in the $\pi\mathbf{9/2}^-[\mathbf{514}]$ band after backbending. This is due to the configuration dependent deformation effects. We do this calculation only to illuminate this. The smaller earlier backbending frequency ω_c in the

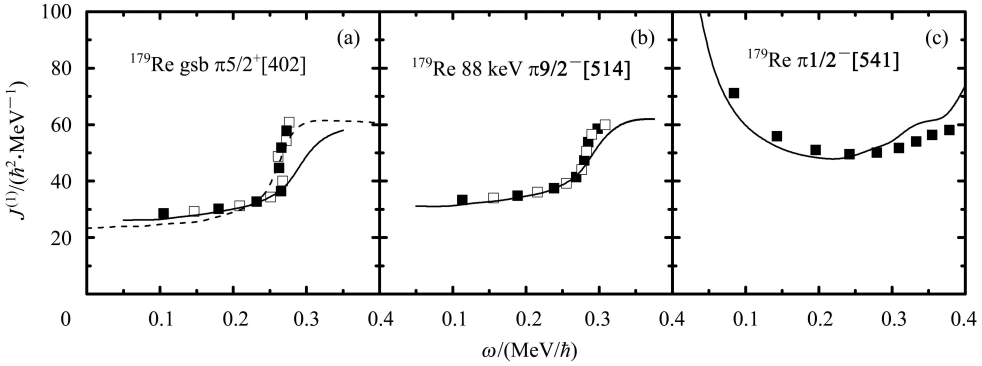

Fig. 2. The MOIs of the low-lying 1-qp bands in ^{179}Re. The experimental MOIs are denoted by ■ ($\alpha = 1/2$) and □ ($\alpha = -1/2$). The calculated MOIs by the PNC method are denoted by solid lines ($\alpha = 1/2$) and dotted lines ($\alpha = -1/2$). (a) The MOI for the gsb $K^\pi = 5/2^+$ ($\pi 5/2^+[402]$). The dashed line is the MOI calculated using a little reduced quadrupole deformation ($\varepsilon_2 = 0.22$). (b) The MOI for the 88 keV band, $K^\pi = 9/2^-$ ($\pi\mathbf{9/2}^-[514]$). (c) The MOI for the $K^\pi = 1/2^-$ ($\pi\mathbf{1/2}^-[541]$) band.

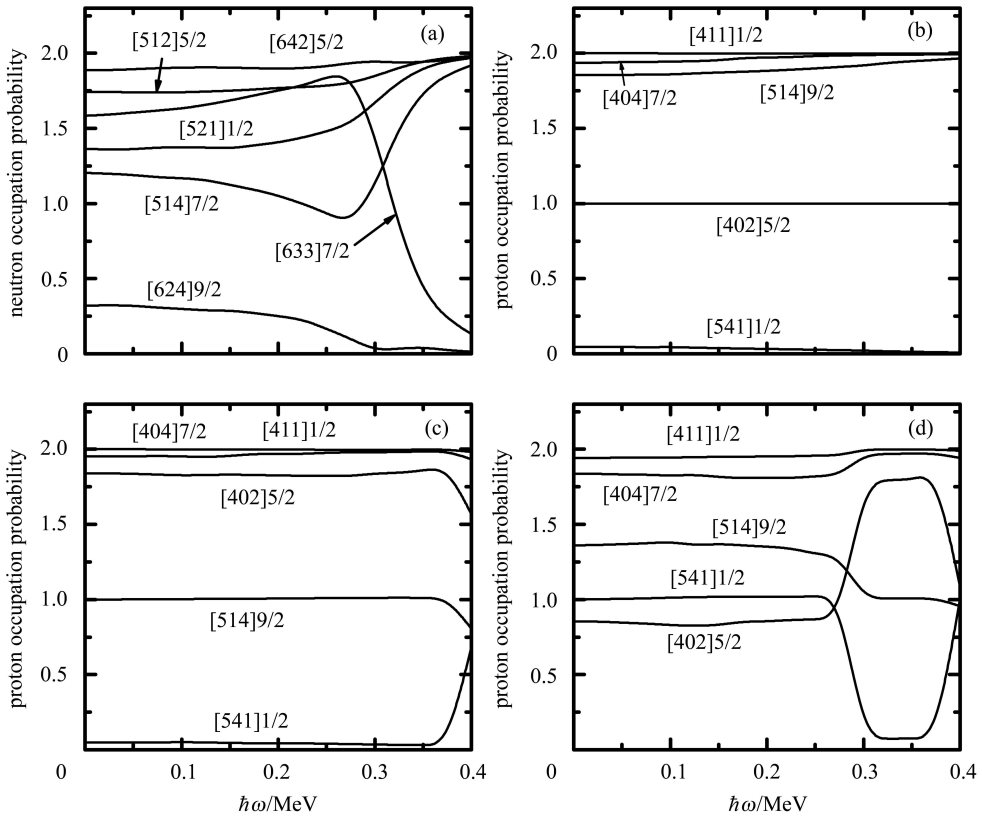

Fig. 3. The occupation probability n_μ for all 1-qp bands in ^{179}Re. (a) The neutron occupation probability for the gsb near the Fermi surface. (b) The proton occupation probability for the gsb $K^\pi = 5/2^+$ ($\pi 5/2^+[402]$). (c) The same as (b) but for the $K^\pi = 9/2^-$ ($\pi\mathbf{9/2}^-[514]$) band. (d) The same as (b) but for the $K^\pi = 1/2^-$ ($\pi\mathbf{1/2}^-[541]$) band. The Nilsson levels far above the Fermi surface ($n_\mu \sim 0$) and levels far below it ($n_\mu \sim 2$) are not shown.

$\pi 5/2^+[402]$ band is also caused by these effects. In Fig. 2(b), the backbending of the $K^\pi = 9/2^-$ ($\pi\mathbf{9/2}^-[514]$) band is reproduced well by our calculation. The backbending in these two bands is caused by a pair with $\nu i_{13/2}$. In Fig. 2(c), because the $K^\pi = 1/2^-$ ($\pi\mathbf{1/2}^-[541]$) band has very strong deformation driving effects in the rare-earth region, many experiments find that the deformation is $\sim$15%–20% larger than that in the gsb [12, 20]. Here, we choose $\varepsilon_2 = 0.252$ for the $\pi\mathbf{1/2}^-[\mathbf{541}]$ band, proving that our calculations can reproduce these effects well. This in turn confirms the deformation driving effects in ^{179}Re.

We present the occupation probability for all 1-qp bands in Fig. 3. The Nilsson levels far above the Fermi surface ($n_\mu \sim 0$) and those far below it ($n_\mu \sim 2$) are not shown. Fig. 3(a) is the neutron occupation probability for the gsb near the Fermi surface. We can see that the occupation probability of $\nu\mathbf{7/2}^+[\mathbf{633}]$ ($i_{13/2}$) drops suddenly down from 1.8 to nearly zero when increasing the cranking frequency ω from 0.27 MeV/$\hbar$ to 0.40 MeV/$\hbar$, and that of the $7/2^-[514]$ increases from 1.0 to nearly 2. So it is understandable that the backbending in both the $\pi 5/2^+[402]$ and the $\pi\mathbf{9/2}^-[\mathbf{514}]$ bands is caused by the crossing of the gsb with a pair of high-j intruder neutron $i_{13/2}$ bands. Fig. 3(b) is the proton occupation probability for the gsb $\pi 5/2^+[402]$. Fig. 3(c) and (d) are the same as Fig. 3(b), but for the proton occupation probability of $\pi\mathbf{9/2}^-[\mathbf{514}]$ and $\pi\mathbf{1/2}^-[\mathbf{541}]$. It should be noted that the concept of "blocked levels" only has a vague meaning even at the bandhead. For example, for the $K^\pi = 1/2^-$ ($\pi\mathbf{1/2}^-[\mathbf{541}]$) band, the orbitals above the Fermi surface ($\pi\mathbf{1/2}^-[\mathbf{541}]$, etc.) are also partially occupied, whereas the orbitals below the Fermi surface ($\pi 5/2^+[402]$) are partially empty (see Fig. 3(d)).

3.3 The 3- and 5-qp bands in ^{179}Re

The experimental $J^{(1)}$s of four low-lying excited high-K 3-qp and three 5-qp bands in ^{179}Re [3, 12] are shown in Fig. 4 by ■ ($\alpha = 1/2$) and □ ($\alpha = -1/2$), and the calculated $J^{(1)}$s are shown by solid ($\alpha = 1/2$) and dotted ($\alpha = -1/2$) lines. Most of these bands are reproduced well by PNC calculation, except the $K^\pi = 17/2^+$ band. It seems strange that this band has no high-j intruder orbital, but has a significantly large MOI. An interaction with a close lying band may paly a role [3]. The anomaly of this band needs further investigation by experiment. The difference between the two high-K 3-qp bands $K^\pi = 15/2^-$ and $K^\pi = 19/2^+$ is that the blocked normal neutron orbital $\nu 7/2^-[514]$ in the former is replaced by the high-j intruder orbital $\nu\mathbf{9/2}^+[\mathbf{624}]$ in the latter. Thus we can understand why $J^{(1)}(K^\pi = 19/2^+)$ is a little larger than $J^{(1)}(K^\pi = 15/2^-)$. All three 5-qp bands contain two high-j intruder neutron orbitals $\nu\mathbf{7/2}^+[\mathbf{633}]$ and $\nu\mathbf{9/2}^+[\mathbf{624}]$, so the magnitude of their $J^{(1)}$s looks the same. No signature splitting is found in of all these 3-qp and 5-qp bands.

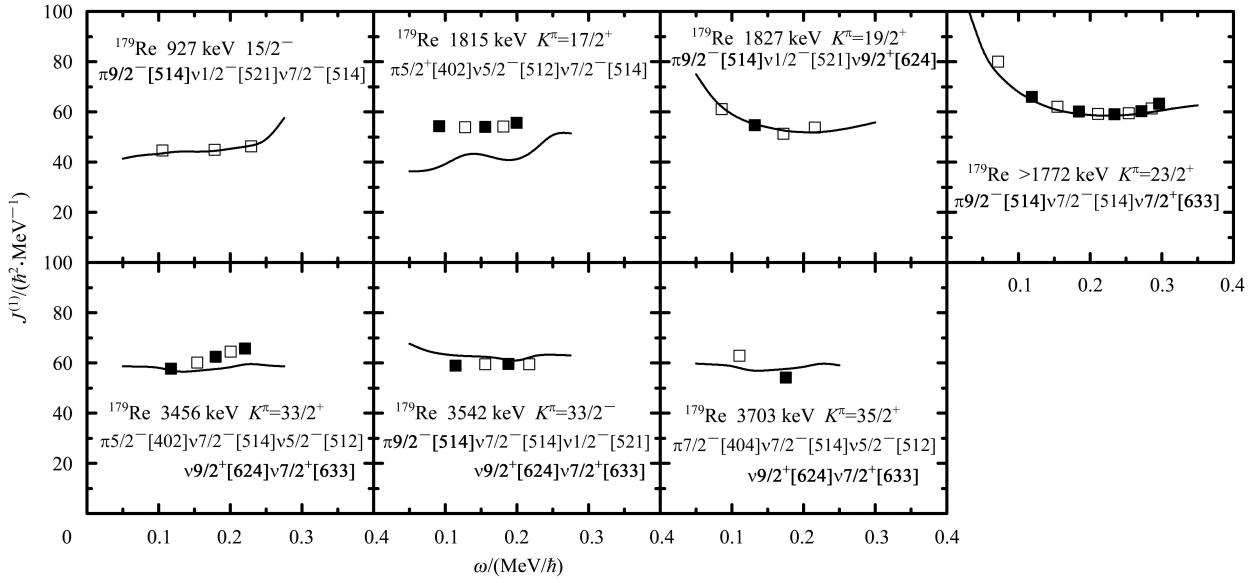

Fig. 4. The same as Fig. 2 but for the low-lying 3-qp and 5-qp bands in ^{179}Re.

4 Summary

The experimental 1-qp bands and low-lying high-K 3-qp and 5-qp bands in ^{179}Re are calculated by the PNC method. The Nilsson level scheme (Lund systematics) is slightly adjusted to reproduce the bandhead energies of the 1-qp bands in the PNC calculation. We show that the little difference in the backbending frequencies between all of the 1-qp bands is due to the different deformation in these bands, which confirms the configuration dependent deformation in the Re nuclei [7]. This is the first time we have used the PNC method to treat the transitional Re nuclei. The experimental $J^{(1)}$s for most bands are reproduced quite well by our calculations, which in turn confirms the configuration assignments for these bands [3, 11].

The authors are grateful to Jin-Yan Zeng, En-Guang Zhao and Shan-Gui Zhou for fruitful discussions.

References

1 Walker P M, Draculis G. Nature, 1999, **399**: 35–40
2 Singh S, Malik S S, Jain A K, Singh B. Atomic Data and Nuclear Data Tables, 2006, **92**: 1–46
3 Thwaites C et al. Phys. Rev. C, 2002, **66**: 054309
4 LIU Y Z, MA Y J, YANG H T, ZHOU S G. Phys. Rev. C, 1995, **52**: 2514–2519
5 LIU Y Z et al. Phys. Rev. C, 1996, **54**: 719–730
6 Walus W et al. Phys. Scr., 1986, **34**: 710–716
7 Bark R A et al. Nucl. Phys. A, 1989, **501**: 157–187
8 Cardona M A et al. Phys. Rev. C, 1999, **59**: 1298–1315
9 Pearson C J et al. Nucl. Phys. A, 2000, **672**: 301–329
10 Purry C S et al. Nucl. Phys. A, 2000, **672**: 54–88
11 Venkova Ts et al. Z. Phys. A, 1989, **334**: 385–395
12 Baglin C M. Nucl. Data Sheets, 2009, **110**: 265–506
13 Stephens F S, Simon R S. Nucl. Phys. A, 1972, **183**: 257–284
14 ZENG J Y, JIN T H, ZHAO Z J. Phys. Rev. C, 1994, **50**: 1388-1397
15 XIN X B, LIU S X, LEI Y A, ZENG J Y. Phys. Rev. C, 2000, **62**: 067303–6
16 WU C S, ZENG J Y. Phys. Rev. C, 1989, **39**: 666–670
17 Moligue H, Dudek J. Phys. Rev. C, 1997, **56**: 1795–1813
18 Nilsson S G et al, Nucl. Phys. A, 1969, **131**: 1–66
19 Bengtsson R, Frauendorf S, May F R. Data and Nucl. Data Tables, 1986, **35**: 15–122
20 Chamoli S K et al. Phys. Rev. C, 2004, **69**: 034310